

From cells to tissue: A continuum model for epithelial mechanics

Shuji Ishihara,^{1,*} Philippe Marcq,² and Kaoru Sugimura^{3,4}

¹*Department of Physics, School of Science and Technology,
Meiji University, Kanagawa 214-8571, Japan*

²*Sorbonne Universités, UPMC Université Paris 6, Institut Curie,
CNRS, UMR 168, Laboratoire Physico Chimie Curie, Paris, France*

³*Institute for Integrated Cell-Material Sciences (WPI-iCeMS),
Kyoto University, Kyoto 606-8501, Japan*

⁴*JST PRESTO, Tokyo 102-0075, Japan*

Abstract

A continuum model for epithelial tissue mechanics is formulated from cell level mechanical ingredients and morphogenetic cell dynamics, including cell shape changes and cell rearrangements. The model is capable of dealing with finite deformation, and uses stress and deformation tensors that can be compared with experimental data. Using the model, we uncover the dynamical behaviour that underlies passive relaxation and active contraction-elongation of a tissue. The present work provides an integrated scheme for understanding the mechanisms by which morphogenetic processes of each individual cell collectively lead to the development of a large tissue with its correct shape and size.

*Electronic address: shuji@meiji.ac.jp

During tissue morphogenesis, tissues acquire their unique shape and size through a series of deformations. Morphogenesis proceeds at multiple scales and each of the molecular, cellular, and tissue scales reciprocally feeds back on the other ones. At the cell level, tissue deformation is accounted for by changes in cell shape, cell position, and cell number (Fig. 1(a, b): hereafter called cell processes), which are triggered by biochemical signaling and forces acting between the cells [1–3]. The activity and localization of signaling and force-generating molecules can be under the control of tissue stress, which consists of forces generated by molecular activities and stress generated by cell processes [4–10]. However, the mechanism by which the shape of a tissue emerges from these multi-scale feedback regulations remains unclear.

Answering this question requires a coarse-grained description and modeling of cell and tissue dynamics at an appropriate length scale: whereas the position and timing of cell processes are stochastic at the cell level, averaging over a larger length scale yields a smooth spatial pattern. We previously determined the appropriate averaging length scale for epithelial tissue dynamics (several tens of cells in a patch), and developed coarse-grained measurement methods for stress and kinematic fields [11–14]. A force inference method quantifies cell junction tensions and cell pressures, which can be integrated to calculate a stress tensor [13–16]. A texture tensor formalism measures morphogenetic behaviours of each individual cell in the same physical dimension, which can be integrated to obtain tissue scale, spatio-temporal maps of cell processes [12]. Together, these methods provide the amplitude, orientation and anisotropy of tissue stress, tissue growth, and cell processes, and correlations between them [12].

A modeling scheme capable of accommodating the quantitative data described above is however still lacking [17]. Cell-based models such as the cell vertex model (CVM) [18] and the cellular Potts model (CPM) [19] are often employed to simulate epithelial development, but the relationship between cell processes and tissue scale deformation and rheology emerges from numerical simulations without being directly tractable. Continuum models allow in-depth analysis of tissue rheology [1, 20], yet in many cases ignore the cellular structure by construction, and thus fail to discriminate different cell processes. A limited number of studies have considered the degrees of freedom that represent cell processes and cell polarity [1, 22–24], but in the context of macroscopic models that do not incorporate cell-level mechanical parameters explicitly. A continuum model has been derived from the CVM

in [25], but without considering cell rearrangements.

Here, we develop a two-dimensional hydrodynamic model of epithelial tissues that connects cell and tissue scales. We start from an energy function used in CVM/CPM to derive the elastic stress, and separate tissue deformation caused by cell shape change from that caused by cell rearrangement. We combine kinematic relationships with the thermodynamic formalism, and determine a hydrodynamic description of the tissue based on stress and deformation tensors that can be compared with experimental data [12–14]. Finally, we solve the model in several conditions typical of deforming planar tissues during development.

Energy function and elastic stress— In CVM and CPM, epithelial tissue is often treated in 2D, and cell geometry is determined by minimizing an energy function such as [26]

$$f_c = \sum_i \frac{K}{2} (A_i - A_0)^2 + \sum_{[ij]} \gamma_0 \ell_{ij} + \sum_i \frac{\kappa_0}{2} L_i^2, \quad (1)$$

where A_i and L_i are the area and perimeter of cell i , and ℓ_{ij} is the length of the interface between cells i and j . The first term represents cell-area elasticity with elastic modulus K and reference cell area A_0 . The second and third terms represent cell junction tension, where the tension in cell i is given by $\gamma_0 + \kappa_0 L_i$.

To construct a continuum model, we first fit each cell by an ellipse, characterized by a 2×2 symmetric tensor S : the cell shape is expressed as $(\vec{r} - \vec{r}_c)^T S^{-T} S^{-1} (\vec{r} - \vec{r}_c) = 1$, where \vec{r}_c is the center of a cell and T denotes the transpose. Since the eigenvalues of S are the lengths of the semi-axes of the ellipse, the cell area is given by $A = \pi |S|$, where $|S|$ is the determinant of S . The cell peripheral length is approximately $L \simeq \hat{\pi} \text{Tr } S$, where $\text{Tr } S$ is the trace of S , and the coefficient $\hat{\pi}$ is approximately equal to π . Close to isotropic conditions, a given cell i has approximately equal cell-junction lengths, $\ell_{ij} \simeq \hat{\pi} \text{Tr } S_i / 6$. Upon coarse-graining, we deduce the elastic energy density per unit area F from Eq. (1) as

$$F = \frac{1}{\pi |S|} \left[\frac{K}{2} (\pi |S| - A_0)^2 + \frac{\gamma_0}{2} \hat{\pi} \text{Tr } S + \frac{\kappa_0}{2} (\hat{\pi} \text{Tr } S)^2 \right] \quad (2)$$

By taking the cell ellipses S as a smooth tensor field $S(\vec{r})$ that represents the cell shape at the position \vec{r} , the total elastic energy is obtained by integration $\mathcal{F} = \int F(S(\vec{r})) \, d\vec{r}$. Importantly, this procedure can be implemented on segmented images of 2D epithelia to

yield an experimental measurement of the field $S(\vec{r})$.

Given Eq. (2), the elastic stress σ_e reads

$$\sigma_e = K(\pi|S| - A_0)I + \frac{\hat{\pi}\gamma_0 + 2\hat{\pi}^2\kappa_0 \text{Tr } S}{2\pi|S|}S, \quad (3)$$

where I is the unit tensor (see Supplemental data for derivation of σ_e). The first and second terms represent respectively the isotropic pressure due to the area-elasticity of cells, and the cell-shape dependent stress due to cell junction tensions. Eq. (3) is consistent with that of the Batchelor stress tensor [28] used in cell-based expression of tissue stress [13, 14].

It is useful to factorize the shape tensor S as $S = S_0 e^C$, where S_0 is a scalar and C is a symmetric, trace-less tensor ($\text{Tr } C = 0$) parametrized by the scalar $c = C_{11} = -C_{22}$. S_0 quantifies the cell area, since $A = \pi|S| = \pi S_0^2$, and C is a dimensionless tensor characterizing cell shape anisotropy. The energy per cell, $A F(A, c = 0)$, is shown as a function of A in Fig. 2(a) in the isotropic case $c = 0$. For large values of γ_0 , the functional form becomes concave, indicating thermodynamic instability of the state of homogeneous cell area. Fig. 2(b) shows $F(A = A_0, c)$ as a function of c at constant cell area A_0 . Circular cell shape ($c = 0$) becomes unstable for large enough negative values of γ_0 , where cells no longer prefer a hexagonal configuration, but adopt an elongated shape. These two instabilities coincide with those known in the CVM [26, 27] (Fig. 2(c); Supplemental data). Therefore, the tissue scale energy density $F(S)$ retains the essential features of the original cell-based models. Below, we use cell mechanical parameters for which the ground state corresponds to a circular shape, allowing coarse-graining since the characteristic length of variation of cell shape is then longer than a cell size.

Kinematics — We defer a study of the effect of cell divisions and cell deaths to future work and consider a situation where individual cells only deform and/or intercalate. The total deformation rate tensor $\nabla \vec{v}$ is the sum of its symmetric part $D = (\nabla \vec{v} + [\nabla \vec{v}]^T)/2$ and antisymmetric part $\Omega = (\nabla \vec{v} - [\nabla \vec{v}]^T)/2$. We decompose D into the sum of contributions respectively due to cell shape changes D_s and cell rearrangements D_r :

$$\nabla \vec{v} = \Omega + D_s + D_r. \quad (4)$$

Since tissue deformation solely by cell rearrangements is irrotational with no tissue area change (*i.e.*, pure shear), D_r is a symmetric and trace-less tensor. One can show that the condition $\text{Tr } D_r = 0$ ensures the conservation of cell number density $\rho = 1/\pi|S|$ in the absence of cell divisions and deaths, $\partial_t \rho + \nabla \cdot (\rho \vec{v}) = 0$. In analogy with the texture tensor [12], we introduce a tensor $M = SS^T$, with the physical dimension of square length. The quantity $\Omega + D_s = \nabla \vec{v} - D_r$ represents the tissue deformation rate by cell shape changes and is kinematically associated with cell shape changes as [1]:

$$\dot{M} - (\nabla \vec{v} - D_r)M - M(\nabla \vec{v} - D_r)^T = 0, \quad (5)$$

where $\dot{M} \equiv \partial_t M + \vec{v} \nabla M$ is the Lagrange derivative of M . The kinematic relationship (31) is known as non-affine deformation in the rheology of foams [29, 30] and polymer melts [31], where D_r is interpreted as due to the slippage between bubbles and between polymer molecules, respectively. Without rearrangements ($D_r = 0$), the left hand side of Eq. (31) becomes the co-deformational (upper-convected) derivative as expected [32].

Thermodynamic formalism — Since existing cell-based models, including CVM and CPM, use *ad hoc* prescriptions for kinetics, we turn to the thermodynamic formalism [33] to derive generic hydrodynamic equations that include dissipative processes. The total stress tensor σ is given by the sum of elastic and dissipative stresses, as

$$\sigma = \sigma_e + \sigma_p. \quad (6)$$

The entropy production rate of an isothermal process is calculated as [34]:

$$T \dot{s} = \sigma : D - \sigma_e : D_s = \sigma_p : D + \sigma_e : D_r, \quad (7)$$

where s is the entropy density, and T is the temperature. Here and below, $a:b$ denotes the scalar product of two arbitrary tensors a and b , $a:b \equiv \sum_{i,j} a_{ij} b_{ij}$, and $a' = a - (\text{Tr } a/2)I$ is the deviatoric part of a . Because D_r is trace-less, we can replace σ_e by σ'_e in Eq. (7). By identifying conjugate flux-force pairs as $\sigma_p \cdot D$ and $D_r \cdot \sigma'_e$, the fluxes (σ_p, D_r) are given by

linear combinations of the forces (D, σ_e') :

$$\sigma_p = \chi^{ss}D - \chi^{sr}\sigma_e', \quad (8)$$

$$D_r = \chi^{rs}D + \chi^{rr}\sigma_e'. \quad (9)$$

The coefficients $\chi^{ss}, \chi^{sr}, \chi^{rs}$, and χ^{rr} are fourth-order tensors that satisfy Onsager's reciprocity (*e.g.*, $\chi_{ijkl}^{sr} = \chi_{klji}^{rs}$). Note that Maxwell's model is obtained for $\chi^{ss} = \chi^{sr} = 0$ ($\sigma = \sigma_e, \sigma_p = 0$), and that Kelvin-Voigt's model is obtained for $\chi^{rs} = \chi^{rr} = 0$ ($D_r = 0$).

The term $\chi^{ss}D$ characterizes intra-cellular dissipative stress due to cell shape change. The relaxation time for cell shape change is much shorter (< minute) than that of cell rearrangement (tens of minutes to hours) [3, 17]. Focusing on longer time scale at which cell rearrangement dominates tissue deformation, we set $\chi^{ss} = 0$ in this study.

Including lowest-order non-linearities, the coupling coefficients χ can depend on S' . Under the condition that D_r is trace-less, the generic form of the force-flux relationships is given as:

$$\sigma_p = -\nu_1\sigma_e' - \nu_2(\sigma_e'S' + S'\sigma_e') - \nu_3(\sigma_e':S')I, \quad (10)$$

$$\begin{aligned} D_r = & \nu_1D' + \nu_2(DS' + S'D - \text{Tr}(DS')I) + \nu_3(\text{Tr } D)S' \\ & + \eta_1^{-1}\sigma_e' + \eta_2^{-1}(\sigma_e'S' + S'\sigma_e' - \text{Tr}(\sigma_e'S')I), \end{aligned} \quad (11)$$

where the coupling coefficients are scalar in an isotropic system. The first three terms in Eq. (35) are called diffusive. The term ν_1D' plays a role similar to the Gordon-Schowalter process [32], with a dimensionless coefficient $\nu_1 \in [0, 1]$. The last two terms in Eq. (35) are called convective, and the positive coefficient η_1 has the dimension of viscosity. They underlie the Maxwellian dynamics.

Finally, we close the system of equations with the force balance equation

$$\nabla \cdot \sigma = f_{\text{ext}} \quad (12)$$

where f_{ext} represents the external force field, supplemented with appropriate boundary conditions. Collectively, the constitutive equations (3,6,34,35) with the kinematic relationships (4,31) and the force balance equation (12) determine hydrodynamic equations for the tissue.

We study below three simple examples of dynamical behaviour predicted by our model, first the passive response following axial stretch by an external force, second the relaxation for the energy with the direction-dependent junction tension, third the deformation of a tissue due to active internal forces.

Passive relaxation upon axial stretching— This example is motivated by observations in the *Drosophila* pupal wing, in which external force from the proximal part of the body stretches the wing along the proximal-distal (PD) axis. Upon tissue stretching, wing cells elongate along the PD axis, then the tissue relaxes when cells intercalate and adopt a less elongated shape over a time scale of several hours [5, 6, 12, 38].

For simplicity sake, we consider an incompressible tissue (S_0 constant, see Supplemental data) with an initial size $L_x \times L_y = L_0 \times L_0$ and in an isotropic, uniform state where the shape tensor is $S = S_0 I$. From time $t = 0$, the tissue is uniformly deformed, elongates along the x -axis at the constant rate $\dot{L}_x/L_x = \partial_x v_x = \lambda$, and consequently contracts along the y -axis at the rate $\dot{L}_y/L_y = \partial_y v_y = -\lambda$ (Fig. 3(a)). When the tissue size becomes $aL_0 \times a^{-1}L_0$, the stretch is stopped. We look for a uniform solution to the problem, so that Eq. (12) is automatically verified when $f_{\text{ext}} = 0$. Under these conditions, the trace-less tensor C , with $c = C_{xx} = -C_{yy}$, is also diagonal. Using Eq. (31), the time evolution of c reads

$$\dot{c} = (1 - \nu_1) \partial_x v_x - \eta_1^{-1} \Gamma(c) \sinh c, \quad (13)$$

where $\Gamma(c) = (\hat{\pi}\gamma_0 + 4\hat{\pi}^2\kappa_0 S_0 \cosh c) / (2\pi S_0)$ depends on cell mechanical properties through γ_0 and κ_0 .

Setting $a = 5$, the time course of cell shape anisotropy $c(t)$ is shown for several values of λ in Fig. 3(b). When $|c| \ll 1$, the temporal evolution becomes Maxwellian,

$$\dot{c} + \eta_1^{-1} \Gamma(0) c = (1 - \nu_1) \partial_x v_x \quad (14)$$

with a characteristic time scale for cell rearrangements $\tau_r = \eta_1 \Gamma(0)^{-1}$. If the stretch rate is slower than this time scale ($\tau_r < \lambda^{-1}$), the cells remain nearly circular during cell rearrangement, which is in a sharp contrast to transient cell elongation for faster tissue stretch.

The energy with biased tension— Since the strength of cell junction tension often depends on a direction dictated by cell and tissue polarity signaling [1, 3, 11], we here introduce an additional term $\gamma_s Q : S/\pi|S|$ to $F(S)$. The directional information is represented by the nematic tensor $Q = \vec{n} \otimes \vec{n} - \text{Tr}(\vec{n} \otimes \vec{n})/2$, where \vec{n} is a unit vector.

Let us consider a uniform and fixed signal $\vec{n} = (0, 1)^T$. For an incompressible and uniformly deformed tissue, Eq. (13) becomes

$$\partial_x v_x = -\partial_y v_y = \frac{\dot{c}}{1 - \nu_1} + \frac{H(c)}{\eta_1(1 - \nu_1)} \quad (15)$$

where $H(c) = \Gamma(c) \sinh c - \frac{\gamma_s}{\pi S_0} \cosh c$ (Supplemental data). In an isotropic stress environment, as may be set by boundary conditions, the system relaxes to an equilibrium state at which the tissue flow stops ($\partial_x v_x = \dot{c} = 0$) and the cell shape is elongated along the x -axis ($c > 0$). During the relaxation, \dot{c} and $H(c)$ can have opposite signs: cells may elongate along an axis along which the tissue is contracted by cell intercalation (Fig. S1; see Sec. 6.2 in Supplemental data).

Active tissue contraction-elongation — Contraction-elongation (CE) denotes simultaneous shrinkage and expansion of a tissue along two orthogonal axes [35]. Motivated by observations of active CE driven by the anisotropic localization of myosin [1, 3, 11], we next study CE driven by the intrinsic activity of the tissue. Following [2], we add the term $r\Delta\mu$ to the entropy production rate Eq. (7), where $\Delta\mu$ is the change in chemical potential associated with a chemical reaction that supplies energy to the system, and r is the reaction rate. By identifying r and $\Delta\mu$ as an additional force-flux pair, two types of activities arise. One is an ‘active stress’ added to the constitutive equation for σ_p (Eq. (8)) as $\sigma_a = \chi^{sa}\Delta\mu$. The other is ‘active rearrangement’ added to the constitutive equation for D_r (Eq. (9)) as $D_a = \chi^{ra}\Delta\mu$. Both σ_a and D_a are symmetric second order tensors. As above, a signal field may provide cells with directional information quantified by a nematic tensor Q . In this case, active stress is given by $\sigma_a = \Delta\mu(\alpha_0 I + \alpha_q Q)$, while active rearrangement reads $D_a = -\beta_q \Delta\mu Q$ (Supplemental data). For an incompressible tissue, $\Delta\mu \alpha_0 I$ is absorbed into the pressure term.

Again assuming an isotropic stress environment ($\sigma_{xx} = \sigma_{yy}$) and setting $\vec{n} = (0, 1)^T$, $\partial_x v_x$ is non-zero and the tissue keeps flowing. In spatially homogeneous, steady state conditions,

the tissue deformation rate is calculated as

$$\partial_x v_x = -\partial_y v_y = \frac{\alpha_q \Delta \mu}{2\eta_1(1-\nu_1)^2} + \frac{\beta_q \Delta \mu}{2(1-\nu_1)}. \quad (16)$$

Both the active stress and the active rearrangement drive the contraction along the y -axis and the elongation along the x -axis. Note however that the cell shape anisotropy c depends only on the active stress, as shown in Fig. 4 by plots of $\partial_x v_x$ and c as a function of either the active stress or the active rearrangement parameters.

Discussion — Starting from the elastic energy of cell-based models, we developed a rheological model for epithelia. Advantages of the approach can be summarized as follows. First, the model is designed to connect cell and tissue dynamics. It gives clear insights into many unanswered questions including how cell level mechanical ingredients (*e.g.*, cell area elasticity and cell junction tension) and morphogenetic cell processes (*e.g.*, cell rearrangement) are related to tissue mechanics and deformation. Second, it deals naturally with large deformations. Third, it can incorporate a signal field, for instance the axial tensor Q that orients active stress and cell rearrangement in this study. Fourth, many of the relevant fields can be experimentally measured, including tissue stress, tissue deformation, cell processes, and chemical signaling such as the concentration field of cell polarity molecules or the orientation field describing the spatial distribution of myosins. Once their dynamics are quantitatively characterized by scalar, vector, or tensor variables [5, 6, 11–13, 37, 38], comparison between model predictions and experimental observations will be straightforward.

Our 2D approach can be easily extended to 3D. Other morphogenetic cell processes, *i.e.*, cell growth, cell division and apoptosis, need to be incorporated to the current modeling scheme [39]. Another possible extension of the model regards kinetics. Here, associated dissipation coefficients were determined phenomenologically. This point can be further explored by considering detailed processes at the cell level.

In conclusion, the present work provides an integrated scheme for understanding mechanical control of epithelial morphogenesis. Feedback between biochemical signaling and mechanics via mechanosensing of a cell [4–8] is one among research directions to pursue.

Acknowledgments

We thank François Graner, Boris Guirao, and Yohanns Bellaïche for discussion. This research was supported by JSPS KAKENHI Grant Number JP24657145 and JP25103008, and by the JSPS Sakura program. S.I. is supported by JST CREST.

- [1] C. P. Heisenberg and Y. Bellaïche, *Cell* **153**, 948 (2013).
- [2] A. Sampathkumar, A. Yan, P. Krupinski, and E. M. Meyerowitz, *Curr. Biol.* **24**, R475 (2014).
- [3] C. Guillot and T. Lecuit, *Annu. Rev. Cell Dev. Biol.* **27**, 157 (2011).
- [4] G. B. Blanchard and R. J. Adams, *Curr. Opin. Genet. Dev.* **21**, 653 (2011).
- [5] B. Aigouy, R. Farhadifar, D. B. Staple, A. Sagner, J. C. Röper, F. Jülicher, and S. Eaton, *Cell* **142**, 773 (2010).
- [6] K. Sugimura and S. Ishihara, *Development* **140**, 4091 (2013).
- [7] W. Y. Aw, B. W. Heck, B. Joyce, and D. Devenport, *Curr. Biol.* **26**, 2090 (2016).
- [8] M. Uyttewaal, A. Burian, K. Alim, B. Landrein, D. Borowska-Wykröt, A. Dedieu, A. Peaucelle, M. Ludynia, J. Traas, A. Boudaoud et al., *Cell* **149**, 439 (2012).
- [9] T. Schluck, U. Nienhaus, T. Aegerter-Wilmsen, and C. M. Aegerter, *PLoS One* **8**, e76171 (2013).
- [10] T. P. Wyatt, A. R. Harris, M. Lam, Q. Cheng, J. Bellis, A. Dimitracopoulos, A. J. Kabla, G. T. Charras, and B. Baum, *Proc. Nat. Acad. Sci. USA* **112**, 5726 (2015).
- [11] F. Bosveld, I. Bonnet, B. Guirao, S. Tlili, Z. Wang, A. Petitalot, R. Marchand, P.-L. Bardet, P. Marcq, F. Graner, and Y. Bellaïche, *Science* **336**, 724 (2012).
- [12] B. Guirao, S. U. Rigaud, F. Bosveld, A. Bailles, J. Lopez-Gay, S. Ishihara, K. Sugimura, F. Graner, and Y. Bellaïche, *eLife* **4**, e08519 (2015).
- [13] S. Ishihara and K. Sugimura, *J. Theor. Biol.* **313**, 201 (2012).
- [14] S. Ishihara, K. Sugimura, S. J. Cox, I. Bonnet, Y. Bellaïche, and F. Graner, *Eur. Phys. J. E* **36**, 45 (2013).
- [15] K. K. Chiou, L. Hufnagel, and B. I. Shraiman, *PLoS Comput. Biol.* **8**, e1002512 (2012).
- [16] G. W. Brodland, J. H. Veldhuis, S. Kim, M. Perrone, D. Mashburn, and M. S. Hutson, *PLoS*

One **9**, e99116 (2014).

- [17] N. Khalilgharibi, J. Fouchard, P. Recho, G. Charras, and A. Kabla, *Curr. Opin. Cell Biol.* **42**, 113 (2016).
- [18] H. Honda, *Int. Rev. Cytol.* **81**, 191 (1983).
- [19] F. Graner and Y. Sawada, *J. Theor. Biol.* **164**, 477 (1993).
- [20] Y. C. Fung, *Biomechanics Mechanical Properties of Living Tissues 2nd ed.* (Springer-Verlag New York, 1993).
- [21] S. Tlili, C. Gay, F. Graner, P. Marcq, F. Molino, and P. Saramito, *Eur. Phys. J. E* **38**, 33 (2015).
- [22] B. I. Shraiman, *Proc. Nat. Acad. Sci. USA* **102** 3318 (2005).
- [23] J. Ranft, M. Basan, J. Elgeti, J. F. Joanny, J. Prost, and F. Jülicher, *Proc. Nat. Acad. Sci. USA* **107**, 20863 (2010).
- [24] M. Popović, A. Nandi, M. Merkel, R. Etournay, S. Eaton, F. Jülicher, and G. Salbreux, *arXiv:1607.03304v1* (2016).
- [25] N. Murisic, V. Hakim, I. G. Kevrekidis, S. Y. Shvartsman, and B. Audoly, *Biophys. J.* **109**, 154 (2015).
- [26] R. Farhadifar, J. C. Röper, B. Aigouy, S. Eaton, and F. Jülicher, *Curr. Biol.* **17**, 2095 (2007).
- [27] D. B Staple, R Farhadifar, J. C. Röper, B Aigouy, S Eaton, and F Jülicher, *Eur. Phys. J. E* **33**, 117 (2010).
- [28] G. K. Batchelor, *J. Fluid Mech.* **41**, 545 (1970).
- [29] P. Marmottant, C. Raufaste, and F. Graner, *Eur. Phys. J. E* **25**, 371 (2008).
- [30] S. Bénito, C. H. Bruneau, T. Colin, C. Gay, and F. Molino, *Eur. Phys. J. E* **25**, 225 (2008).
- [31] R. G. Larson, *Constitutive Equations for Polymer Melts and Solutions* (Butterworth-Heinemann, 1988).
- [32] R. G. Larson, *J. Non-Newton. Fluid Mech.* **13**, 279 (1983).
- [33] S. R. De Groot and P. Mazur, *Non-equilibrium Thermodynamics* (North-Holland Publishing Company, Amsterdam, 1962).
- [34] A. I. Leonov, *Rheologica Acta* **15**, 85 (1976).
- [35] M. Tada and C. P. Heisenberg, *Development* **139**, 3897 (2012).
- [36] K. Kruse, J. F. Joanny, F. Jülicher, J. Prost, and K. Sekimoto, *Eur. Phys. J. E* **16**, 5 (2005).
- [37] G. B. Blanchard, A. J. Kabla, N. L. Schultz, L. C. Butler, B. Sanson, N. Gorfinkiel, L.

Mahadevan, and R. J. Adams, *Nat. Methods* **6**, 458 (2009).

[38] R. Etournay, M. Popović, M. Merkel, A. Nandi, C. Blasse, B. Aigouy, H. Brandl, G. Myers, G. Salbreux, F. Jülicher et al., *eLife* **4**, e14334 (2015).

[39] S. Yabunaka and P. Marcq, Preprint (2016).

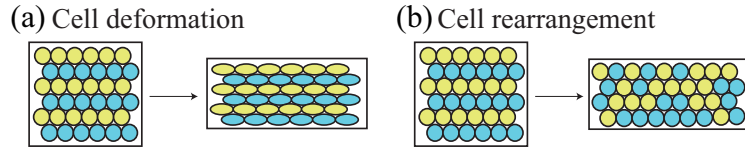


FIG. 1: (a) Tissue deformation by cell shape deformation, without cell rearrangement. (b) Tissue deformation by cell rearrangement, without cell shape deformation.

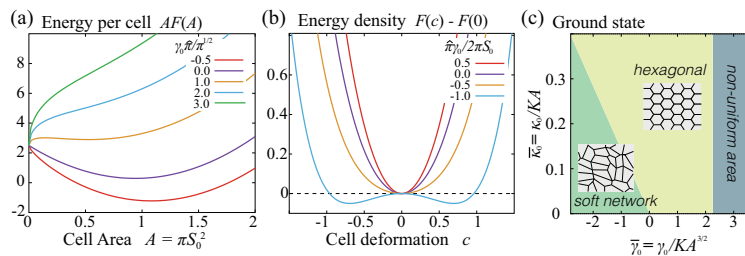


FIG. 2: (a) Energy per cell as a function of the cell area A at $\gamma_0 \hat{\pi} / \pi^{1/2} = -0.5, 0.0, 1.0, 2.0$ and 3.0 with $K = 5.0$ and $2\kappa_0 \hat{\pi}^2 / \pi = 0.3$. (b) Energy density function $F(c)$ at $\hat{\pi} \gamma_0 / 2\pi S_0 = 0.5, 0.0, -0.5$, and -1.0 with $2\hat{\pi}^2 \kappa_0 S_0 / \pi = 0.8$. (c) A ground state phase diagram is shown as a function of non-dimensionalized parameters $\bar{\gamma}_0 = \gamma_0 / KA^{3/2}$ and $\bar{\kappa}_0 = \kappa_0 / KA$, defined with a cell area scale $A = \pi S_0^2$ (instead of A_0 [26, 27]).

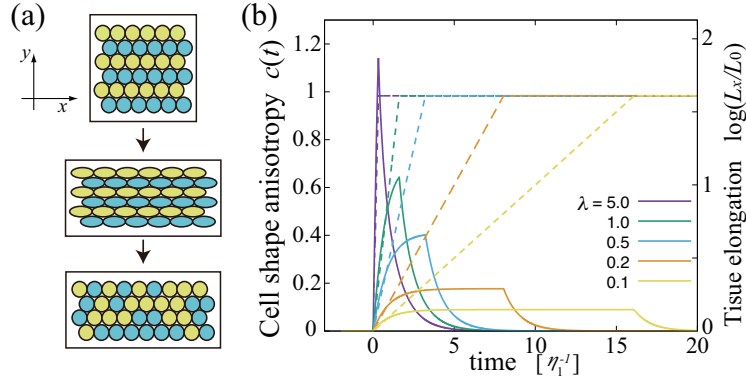


FIG. 3: (a) Stretch along the x -axis of a tissue of constant area. Cells are elongated by the stretch, then relax to recover a circular shape. (b) Cell shape anisotropy $c(t)$ (solid lines). Forced deformation ($a = 5$, dashed lines) with the deformation rates $\lambda = 5.0, 1.0, 0.5, 0.2, 0.1$ is followed by relaxation (numerical solution of Eq. (13)). Parameters are $\hat{\pi}\gamma_0/2\pi S_0 = 0.2$, $2\hat{\pi}^2\kappa_0/\pi = 0.8$, $\nu_1 = 0.1$, and $\eta_1 = 1.0$. The characteristic time is $\tau_r = \eta_1\Gamma(0)^{-1} = 1.0$.

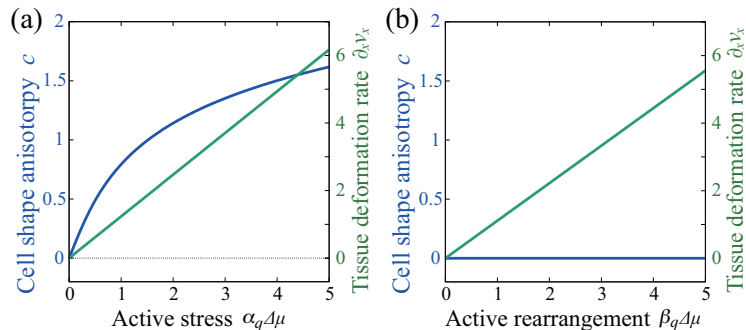


FIG. 4: Dependence of the cell shape anisotropy c and the tissue deformation rate $\partial_x v_x$ on the active parameters: (a) active stress $\alpha_q \Delta \mu$ ($\beta_q = 0$); (b) active rearrangement $\beta_q \Delta \mu$ ($\alpha_q = 0$). Parameter values are the same as in Fig. 3.

Supplemental data

I. STABILITY ANALYSIS

A. Cell area instability

Let cell shape be uniform, not depending on the position \vec{r} . The cell area is taken as $A = \pi S_0^2$, and the energy density function per cell, $f = AF(S)$, is expressed as

$$f = \frac{K}{2} (\pi S_0^2 - A_0)^2 + \frac{\gamma_0}{2} \hat{\pi} S_0 \text{Tr} e^C + \frac{\kappa_0}{2} (\hat{\pi} S_0 \text{Tr} e^C)^2 \quad (17)$$

The pressure P is obtained by differentiating f with respect to A (see also Eq. (28)).

$$P = -\frac{\partial f}{\partial(\pi S_0^2)} = -K(\pi S_0^2 - A_0) - \frac{\gamma_0}{4} \frac{\text{Tr} e^C}{S_0} - \frac{1}{2} \kappa_0 \pi (\text{Tr} e^C)^2. \quad (18)$$

Here, we used $\hat{\pi} = \pi$. Thermodynamic stability holds when $\partial P / \partial A < 0$, which leads to the following condition:

$$\bar{\gamma}_0 \equiv \frac{\gamma_0}{KA^{3/2}} < \frac{8}{\pi^{1/2} \text{Tr} e^C} \quad (19)$$

Note that $\text{Tr} e^C \geq 2$, where the equality holds at $C = 0$. The cell area A depends on parameters and boundary conditions. For a given cell area, the described condition does not hold for large γ_0 values, indicating that the homogenous cell size state is unstable.

B. Cell shape instability

By differentiating Eq. (17) with respect to $\text{Tr} e^C$ while keeping S_0 fixed, we obtain

$$\frac{\partial f}{\partial \text{Tr} e^C} = \frac{\gamma_0}{2} \hat{\pi} S_0 + \kappa_0 \hat{\pi}^2 S_0^2 \text{Tr} e^C \quad (20)$$

Since $\text{Tr} e^C \geq 2$, f takes its minimal value at $C = 0$ as long as $\gamma_0 \hat{\pi} S_0 / 2 + 2\kappa_0 \hat{\pi}^2 S_0^2 > 0$, *i.e.*,

$$\gamma_0 > -4\kappa_0 \hat{\pi} S_0. \quad (21)$$

If γ_0 is smaller than the threshold value $-4\kappa_0 \hat{\pi} S_0$, the circular shape is no longer stable, and cells preferentially take an elongated shape. Using a non-dimensionalized parameter $\bar{\kappa}_0 = \kappa_0 / KA$, the above condition can be written as (using $\hat{\pi} = \pi$ again)

$$\bar{\gamma}_0 > -4\pi^{1/2} \bar{\kappa}_0 \quad (22)$$

II. DERIVATION OF ELASTIC STRESS

Let each material point at the position \vec{r} move to $\vec{r}' = \vec{r} + \vec{u}(\vec{r})$, thus defining the displacement field \vec{u} . The cell shape before the deformation is represented by $(\vec{r} - \vec{r}_c)^T S^{-T} S^{-1} (\vec{r} - \vec{r}_c) = 1$, where \vec{r}_c represents the center of a cell. Using the deformation given by $\vec{u}(\vec{r})$, the center of a cell changes as $\vec{r}'_c = \vec{r}_c + \vec{u}(\vec{r}_c)$ and the cell shape changes as $(\vec{r} - \vec{r}'_c)^T (1 + \nabla \vec{u})^{-T} S^{-T} S^{-1} (1 + \nabla \vec{u})^{-1} (\vec{r} - \vec{r}'_c) = 1$, indicating that $M = S^T S$ changes as

$$M'(\vec{x} + \vec{u}) = (1 + \nabla \vec{u}) M(\vec{x}) (1 + \nabla \vec{u}^T)$$

Therefore, at the order of $\mathcal{O}(|\nabla \vec{u}|)$,

$$M \rightarrow M' = M - \vec{u} \cdot \nabla M + M(\nabla \vec{u})^T + \nabla \vec{u} M \quad (23)$$

This equation represents the relationship between the change in the cell shape and tissue deformation, when no cell rearrangement occurs [1].

By the virtual deformation \vec{u} , the total energy $\mathcal{F}(M) = \int F(M) d\vec{x}$ changes as follows:

$$\begin{aligned} \delta \mathcal{F} &= \mathcal{F}(M') - \mathcal{F}(M) \sim \int \frac{\partial F}{\partial M} : \delta M d\vec{x} \\ &= \int \frac{\partial F}{\partial M} : (-\vec{u} \cdot \nabla M + M(\nabla \vec{u})^T + \nabla \vec{u} M) d\vec{x} \\ &= \int \left[-\nabla \cdot (\vec{u} F) + \left(FI + \left(\frac{\partial F}{\partial M} \right)^T M + \frac{\partial F}{\partial M} M^T \right) : \nabla \vec{u} \right] d\vec{x} \end{aligned}$$

where I represents a unit tensor. The first term vanishes at the boundary of the system, and the elastic stress σ_e is given as:

$$\sigma_e = FI + \left(\frac{\partial F}{\partial M} \right)^T M + \left(\frac{\partial F}{\partial M} \right) M^T \quad (24)$$

Using the relationship

$$\frac{\partial F}{\partial M} : \delta M = \frac{1}{2} \frac{\partial F}{\partial S} S^{-1} : \delta M \quad (25)$$

σ_e can also be written as follows:

$$\sigma_e = FI + \frac{1}{2} S^{-1} \left[\left(\frac{\partial F(S)}{\partial S} \right)^T S + S \left(\frac{\partial F(S)}{\partial S} \right) \right] S. \quad (26)$$

This equation provides the general expression for the stress tensor for a given energy $F(S)$.

For the energy $F(S)$ given in Eq. (2) in the main text, σ_e is calculated as

$$\sigma_e = K(\pi|S| - A_0)I + \frac{\gamma_0\hat{\pi} + 2\kappa_0\hat{\pi}^2\text{Tr } S}{2\pi|S|}S. \quad (27)$$

Note that the pressure is obtained as

$$P = -\frac{1}{2}\text{Tr } \sigma_1 = -K(\pi|S| - A_0) - \frac{\gamma_0\hat{\pi} + 2\kappa_0\hat{\pi}^2\text{Tr } S}{4\pi|S|}\text{Tr } S \quad (28)$$

which coincides with Eq. (18).

III. EQUATIONS FOR TISSUE DEFORMATION

For convenience, we list the equations describing tissue deformation.

a. *Kinematic equations* are given as:

$$\nabla\vec{v} = \Omega + D_s + D_r \quad (29)$$

$$\text{Tr } D_r = 0 \quad (30)$$

$$\dot{M} = (\nabla\vec{v} - D_r)M + M(\nabla\vec{v} - D_r)^T \quad (31)$$

Here, $\Omega = (\nabla\vec{v} - [\nabla\vec{v}]^T)/2$ represents the asymmetric part of the deformation rate tensor, while $D_s + D_r$ represents its symmetric part. D_r represents the deformation rate caused by cell rearrangement, the trace of which is zero.

b. *Constitutive equations* are given as:

$$\sigma = \sigma_e + \sigma_p \quad (32)$$

$$\sigma_e = K(\pi|S| - A_0)I + \frac{\gamma_0\hat{\pi} + 2\kappa_0\hat{\pi}^2\text{Tr } S}{2\pi|S|}S \quad (33)$$

$$\sigma_p = -\nu_1\sigma_e' - \nu_2(\sigma_e'S' + S'\sigma_e') - \nu_3(\sigma_e':S')I, \quad (34)$$

$$\begin{aligned} D_r = & \nu_1D' + \nu_2(DS' + S'D - \text{Tr}(DS')I) + \nu_3(\text{Tr } D)S' \\ & + \eta_1^{-1}\sigma_e' + \eta_2^{-1}(\sigma_e'S' + S'\sigma_e' - \text{Tr}(\sigma_e'S')I), \end{aligned} \quad (35)$$

where σ_e and σ_p are the elastic and dissipative stress, respectively.

To obtain Eqs. (34-35) (Eqs. (10) and (11) in the main text), we set the fourth-order

tensors χ^{sr} and χ^{rr} as follows:

$$\begin{aligned}\chi_{ijkl}^{\text{sr}} &= \nu_1 \left(\delta_{ik} \delta_{lj} - \frac{1}{2} \delta_{ij} \delta_{kl} \right) + \nu_2 \left(\delta_{ik} S'_{lj} + S'_{ik} \delta_{jl} - S'_{ij} \delta_{kl} \right) \\ &\quad + \nu_3 S'_{kl} \delta_{ij}\end{aligned}\quad (36)$$

$$\chi_{ijkl}^{\text{rr}} = \eta_1^{-1} \delta_{ik} \delta_{jl} + \eta_2^{-1} \left(\delta_{ik} S'_{lj} + S'_{ik} \delta_{jl} - S'_{ij} \delta_{kl} \right) \quad (37)$$

χ^{ss} is taken to be zero, and χ_{ijkl}^{rs} is determined by Onsager's reciprocity $\chi_{ijkl}^{\text{rs}} = \chi_{klji}^{\text{sr}}$.

$$\begin{aligned}\chi_{ijkl}^{\text{rs}} &= \nu_1 \left(\delta_{ik} \delta_{lj} - \frac{1}{2} \delta_{ij} \delta_{kl} \right) + \nu_2 \left(\delta_{ik} S'_{lj} + S'_{ik} \delta_{jl} - \delta_{ij} S'_{kl} \right) \\ &\quad + \nu_3 \delta_{kl} S'_{ij}\end{aligned}\quad (38)$$

c. *The force balance equation* reads:

$$\nabla \cdot \sigma = f_{\text{ext}} \quad (39)$$

where f_{ext} represents the external force.

IV. INCOMPRESSIBLE CASE

If the tissue is incompressible, the factorization $S = S_0 e^C$, is useful, where S_0 is constant. From Eq. (31), we obtain the time evolution of S_0 and C :

$$\dot{S}_0 = \text{Tr } D_s \times S_0 / 2 \quad (40)$$

$$\dot{C} = D'_s + \Omega C - C \Omega \quad (41)$$

According to Eq. (40), $\text{Tr } D_s = 0$ must hold to satisfy $\dot{S}_0 = 0$. Additionally, this condition also implies that $\nabla \cdot \vec{v} = \text{Tr } D = \text{Tr } D_s + \text{Tr } D_r = 0$, a general condition for an incompressible fluid.

Eq. (31) is replaced by Eq. (41), which can be written as $\overset{\circ}{C} = D'_s$, in which the co-rotational derivative is defined as $\overset{\circ}{C} \equiv \dot{C} - \Omega C + C \Omega$.

Stress and constitutive equations are replaced by

$$\sigma = \sigma'_e + \sigma'_p - pI, \quad (42)$$

$$\sigma'_e = \frac{\gamma_0 \hat{\pi} + 2\kappa_0 \hat{\pi}^2 S_0 \text{Tr } e^C}{2\pi S_0} [e^C]', \quad (43)$$

$$\sigma'_p = -\nu_1 \sigma'_e - \nu_2 (\sigma'_e S' + S' \sigma'_e) \quad (44)$$

$$D_r = \nu_1 D' + \nu_2 (DS' + S'D - \text{Tr}(DS')I), \\ +\eta_1^{-1} \sigma'_e + \eta_2^{-1} (\sigma'_e S' + S' \sigma'_e - \text{Tr}(\sigma'_e S')I), \quad (45)$$

where p represents the pressure of the system.

V. ACTIVITIES

To include the activities related to the tissue deformation dynamics, we adopted the formalism developed for active gels [2]. A reaction that supplies the energy to the system contributes to the entropy production rate as

$$T\dot{s} = \sigma_p : D + \sigma_e : D_r + r\Delta\mu \quad (46)$$

where r is the reaction rate and $\Delta\mu$ is the reaction-induced change of chemical potential. r and $\Delta\mu$ represent an additional conjugate pair of flux and force. Constitutive equations at the linear order are given as:

$$\sigma_p = \chi^{ss} D - \chi^{sr} \sigma'_e + \chi^{sa} \Delta\mu \quad (47)$$

$$D_r = \chi^{rs} D + \chi^{rr} \sigma'_e + \chi^{ra} \Delta\mu \quad (48)$$

When sustaining the activity, $\Delta\mu$ is fixed, and $\sigma_a = \chi^{sa} \Delta\mu$ and $D_a = \chi^{ra} \Delta\mu$ are the active stress and active rearrangement, respectively.

Considering a signal, such as anisotropic subcellular localization of myosin II, the directionality of the field is characterized by a trace-less tensor Q , where

$$Q = \vec{n} \otimes \vec{n} - \text{Tr}(\vec{n} \otimes \vec{n})/2, \quad (49)$$

and \vec{n} represents a unit vector pointing to the direction θ , as $\vec{n} = (\cos \theta, \sin \theta)^T$. According to (48), D_a is trace-less in the incompressible case. If we assume that the activities depend

on Q , the coefficients χ^{sa} and χ^{ra} become linear functions of Q at lowest order:

$$\sigma_a = \alpha_0 \Delta\mu I + \alpha_q \Delta\mu Q, \quad (50)$$

$$D_a = -\beta_q \Delta\mu Q. \quad (51)$$

VI. PASSIVE AND ACTIVE TISSUE DEFORMATION

A. Contraction-elongation

We considered the deformation of rectangular tissue, with the size $L_x \times L_y$. We assume that the tissue is incompressible and uniformly deformed: $L_x L_y = \text{constant}$ and $\partial_x v_x = \dot{L}_x / L_x = -\partial_y v_y = -\dot{L}_y / L_y$. All tensor variables are diagonal. Cell shape S is designated as $S = S_0 e^C$, where S_0 is constant due to the incompressibility and

$$e^C = \begin{pmatrix} e^c & 0 \\ 0 & e^{-c} \end{pmatrix}. \quad (52)$$

The strength of cell junction tension, $\Gamma(c)$, was defined as:

$$\Gamma(c) \equiv \frac{\hat{\pi}\gamma_0 + 4\hat{\pi}^2\kappa_0 S_0 \cosh c}{2\pi S_0} \quad (53)$$

1. Passive relaxation upon axial tissue stretching

Equations for the axial tissue stretching are given as:

$$\dot{c} = (1 - \nu_1) \partial_x v_x - \eta_1^{-1} \Gamma(c) \sinh c, \quad (54)$$

$$\sigma_{xx} = (1 - \nu_1) \Gamma(c) \sinh c - p, \quad (55)$$

$$\sigma_{yy} = -(1 - \nu_1) \Gamma(c) \sinh c - p. \quad (56)$$

The first equation (54) is the same as Eq. (13) presented in the main text. p represents the pressure, which is determined in order to satisfy the incompressible condition.

2. Anisotropic tension

If the energy function has an additional anisotropic term, $\gamma_s Q : S/\pi|S|$, an additional elastic stress term is included. By using Eq. (26), σ_e can be determined as

$$\sigma_e = K(\pi \det S - A_0)I + \frac{\gamma_0 \hat{\pi} + 2\kappa_0 \hat{\pi}^2 \text{Tr } S}{2\pi \det S}S + \frac{\gamma_s}{2\pi \det S}S^{-1}(QS + SQ)S, \quad (57)$$

where the final term represents the stress associated with the anisotropic tension.

For $\vec{n} = (0, 1)^T$, tissue deformation is governed by the following equations.

$$\dot{c} = (1 - \nu_1)\partial_x v_x - \eta_1^{-1}H(c), \quad (58)$$

$$\sigma_{xx} = (1 - \nu_1)H(c) - p, \quad (59)$$

$$\sigma_{yy} = -(1 - \nu_1)H(c) - p. \quad (60)$$

$$H(c) = \Gamma(c) \sinh c - \frac{\gamma_s}{\pi S_0} \cosh c \quad (61)$$

For an isotropic stress condition ($\sigma_{xx} = \sigma_{yy}$), the system reaches the equilibrium at which $H(c) = 0$, *i.e.*,

$$\Gamma(c) \sinh c = \frac{\gamma_s}{\pi S_0} \cosh c \quad (62)$$

is satisfied and the cell shape is elongated along the x -axis ($\gamma_s > 0$). In Fig 5(a), the equilibrium cell shape anisotropy c for the given γ_s values is presented.

3. Active tissue flow

The active processes are explained in the main text, and the time evolution of c and stresses are given as follows.

$$\dot{c} = (1 - \nu_1)\partial_x v_x - \zeta_1 \Gamma(c) \sinh c + \beta_q \Delta\mu/2 \quad (63)$$

$$\sigma_{xx} = (1 - \nu_1)\Gamma(c) \sinh c - p - \alpha_q \Delta\mu/2 \quad (64)$$

$$\sigma_{yy} = -(1 - \nu_1)\Gamma(c) \sinh c - p + \alpha_q \Delta\mu/2 \quad (65)$$

where α_q and β_q indicate the strength of the active stress and active rearrangement, respectively.

For an isotropic stress condition ($\sigma_{xx} = \sigma_{yy}$), the cell shape is determined by the active stress as:

$$(1 - \nu_1)\Gamma(c) \sinh c = \alpha_q \Delta\mu/2 \quad (66)$$

At the steady state ($\dot{c} = 0$), tissue deformation rate $\partial_x v_x$ does not vanish and the tissue maintains a steady flow through cell intercalation.

B. Case study: the relaxation equation for the energy function with biased cell junction tension

In order to obtain a further insight into the effects of direction-dependent cell junction tension introduced in the energy function (Eqs. (58-60)), here we consider a situation in which the tissue is compressed by the surrounding elastic medium. The following boundary condition is employed.

$$\sigma_{xx} = -k_x \log(L_x/L_x^0) , \quad (67)$$

$$\sigma_{yy} = -k_y \log(L_y/L_y^0) . \quad (68)$$

L_x^0 and L_y^0 are natural lengths of the system along x - and y -axes, respectively. Due to the incompressibility, $L_x L_y$ is constant. Pressure p is determined as

$$p = \frac{1}{2} \left(k_x \log \frac{L_x}{L_x^0} - k_y \log \frac{L_y}{L_y^0} \right) , \quad (69)$$

and therefore, the following relationship holds:

$$-\frac{1}{2} \left(k_x \log \frac{L_x}{L_x^0} - k_y \log \frac{L_y}{L_y^0} \right) = (1 - \nu_1) H(c) \quad (70)$$

Here, $H(c, \gamma_s) \equiv \Gamma(c) \sinh c - (\gamma_s/\pi S_0) \cosh c$ is used. Using a relationship $\partial_x v_x = \dot{L}_x/L_x = -\partial_y v_y = -\dot{L}_y/L_y$, differentiation of Eq. (70) leads to

$$\frac{\dot{L}_x}{L_x} = -\frac{(1 - \nu_1)}{\bar{k}} (H_{\gamma_s} \dot{\gamma}_s + H_c \dot{c}) \quad (71)$$

where $H_{\gamma_s} \equiv \partial H(c, \gamma_s)/\partial \gamma_s$, $H_c \equiv \partial H(c, \gamma_s)/\partial c$, and $\bar{k} \equiv (k_x + k_y)/2$ are used. Eq. (58) becomes:

$$\dot{c} = \frac{-1}{1 + (1 - \nu_1)^2 H_c / \bar{k}} \left(\frac{(1 - \nu_1)^2}{\bar{k}} H_{\gamma_x} \dot{\gamma}_s + \eta_1^{-1} H \right) . \quad (72)$$

Therefore, we obtained

$$\frac{\dot{L}_x}{L_x} = \frac{1 - \nu_1}{\bar{k}} \frac{-H_{\gamma_s} \dot{\gamma}_s + \eta_1^{-1} H_c H}{1 + (1 - \nu_1)^2 H_c / \bar{k}} . \quad (73)$$

Eqs. (72) and (73) describe the time evolution of cell shape anisotropy c and system size L_x .

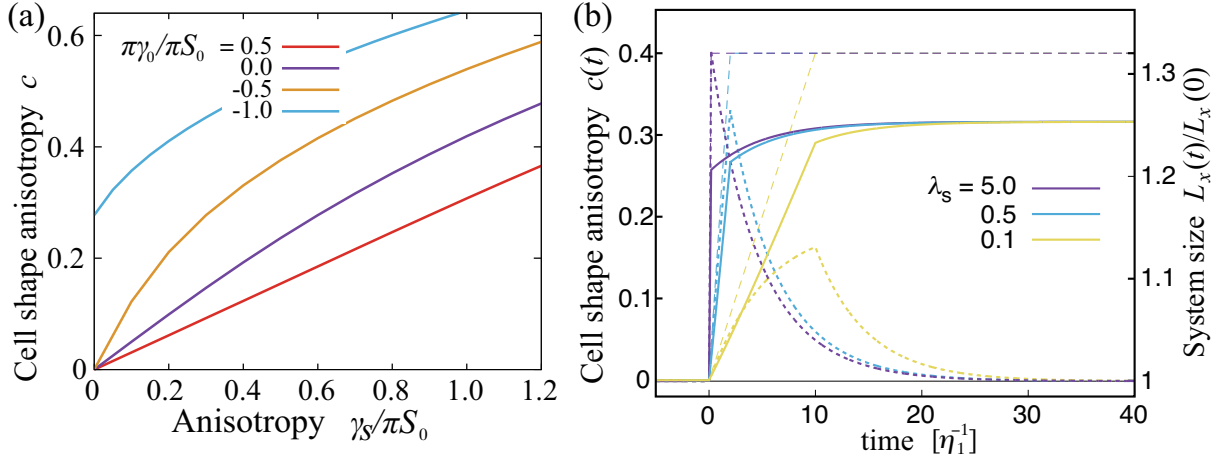


FIG. 5: (a) Cell shape anisotropy at the equilibrium as a function of $\gamma_s/\pi S_0$. $6\hat{\pi}^2\kappa_0 S_0/\pi = 0.8$. (b) Development of cell shape deformation $c(t)$ (solid line) and system size along x -axis $L_x(t)/L_x(0)$ (dotted line). $\gamma_s(t)$ is given as Eq. (74), where γ_0 increases from 0 to $\gamma_s^f = 1.0$. The parameters are set as: $\hat{\pi}\gamma_0/2\pi S_0 = 0.2$, $2\hat{\pi}^2\kappa_0/\pi = 0.8$, $\nu_1 = 0.1$, $\eta_1 = 1.0$, and $\bar{k} = 0.2$.

Consider the case in which γ_s develops as:

$$\gamma_s(t) = \begin{cases} 0 & t < 0 \\ \lambda_s t & 0 \leq t < \gamma_s^f/\lambda_s, \\ \gamma_s^f & \gamma_s^f/\lambda_s \leq t, \end{cases} \quad (74)$$

and the system resides in an isotropic state with the cell shape $c = 0$ for $t < 0$. At time $t = 0$, γ_s starts to increase at the rate λ_s until it reaches γ_s^f , its final constant value.

During the time evolution, \dot{c} is always non-negative and cells elongate along the x -axis. On the other hand, \dot{L}_x can be either positive or negative: In Eq. (73), $-H_{\gamma_s}\dot{\gamma}_s$ is positive, while $\eta_1^{-1}H_cH$ is negative. In Figure 5(b), the time evolution of the cell shape anisotropy $c(t)$ (solid lines) and system size $L_x(t)$ for three different values of λ_s values are shown.

The system reaches its equilibrium at which both the cell deformation and tissue deformation stop occurring ($\dot{c} = \dot{L}_x = 0$). At the equilibrium, c is determined by $H(c^f, \gamma_s^f) = 0$. Equilibrium stress is independent of γ_s , and isotropic ($\sigma_{xx} = \sigma_{yy} = -p$). Accordingly, system size values L_x and L_y at the equilibrium are independent of γ_s in the boundary condition employed here. In numerical simulations, L_x returns to the original length in time (Fig. 5(b)).

[1] S. Tlili, C. Gay, F. Graner, P. Marcq, F. Molino, and P. Saramito, Eur. Phys. J. E **38**, 33 (2015).
[2] K. Kruse, J. F. Joanny, F. Jülicher, J. Prost, K. Sekimoto, Eur. Phys. J. E. **16**, 5 (2005).